



ZnO AND ALKALINE EARTH METAL (Mg) DOPED ZnO NANOPARTICLES FOR ANTIBACTERIAL ACTIVITY, STRUCTURAL AND THERMAL STUDIES

G. Senthamilselvan¹, A. Palanimurugan¹, A. Dhanalakshmi², A. Cyril*¹

¹PG and Research Department of Chemistry, Raja Doraisingam Government Arts College, Sivagangai, Tamil Nadu, India

²PG and Research Department of Physics, Raja Doraisingam Government Arts College, Sivagangai, Tamil Nadu, India

*Corresponding author: cyrilchemistry@gmail.com

Received: 18-09-2021; Revised: 16-02-2022; Accepted: 13-03-2022; Published: 30-04-2022

© Creative Commons Attribution-NonCommercial-NoDerivatives 4.0 International License <https://doi.org/10.55218/JASR.202213329>

ABSTRACT

The chemical co-precipitation method was used to prepare zinc oxide and magnesium doped ZnO nanoparticles (Mg-ZnO NPs), and their structural, optical, thermal, and antibacterial properties were investigated. XRD spectra revealed that all synthesized NPs are hexagonal wurtzite structure and the size of ZnO and Mg-ZnO NPs is 51 and 42 nm. The FTIR spectra of ZnO and Mg-ZnO NPs have peaks at 463 and 470 cm^{-1} respectively. Mg-ZnO NPs have increased the thermal stability region from (177-288°C) to (198-296°C). ZnO NPs have high antibacterial activity against *E. coli*, whereas Mg-ZnO NPs have antibacterial activity against *Pseudomonas aeruginosa*.

Keywords: ZnO, Mg-ZnO, Powder XRD, TGA, Antibacterial activity.

1. INTRODUCTION

Semiconductor materials have drawn attention of the scientists for the past years due to their attracting properties such as optical, structural and morphological. The scientific community considered ZnO NPs to be a promising material for a variety of optoelectronic applications. Various methods have been used to fabricate ZnO nanoparticles such as vapor-phase growth, vapor liquid solid process, a soft chemical method, chemical co-precipitation, homogeneous precipitation, sol gel, electrophoresis deposition, etc [1]. Amongst, the chemical co-precipitation is the suitable method and low cost [2] in the course of a high yield rate used for the preparation of large quantity of ZnO and Mg-ZnO NPs. This study focuses on their synthesis by chemical co-precipitation. It is an environmentally friendly material with high chemical stability and low toxicity. They have been widely used as an active ingredient for dermatological applications due to their antibacterial properties [3]. The properties of the ZnO and Mg-ZnO NPs are suitable for biomedical applications that require precise control of the particle size, shape, and preparation conditions that affect these properties. Various physical or chemical synthesis methods have been used to prepare doped ZnO nanoparticles. To develop optical absorption

properties and achieve small particle sizes, the search for alternative methods for well-organized Mg-ZnO NPs has become a major research interest with high surface areas to better antibacterial by co-precipitation method [4]. The antibacterial efficacy of ZnO and Mg-ZnO NPs was tested against the growth of *Escherichia coli*, *Pseudomonas aeruginosa*, *Staphylococcus aureus*, *Proteus vulgaris* and *Klebsiella pneumoniae* by disc diffusion for 24 h. It is here reported that the influence of structural, morphological, vibrational and thermal studies of NPs was also investigated on their antibacterial activities.

2. MATERIAL AND METHODS

2.1. Materials, Synthesis of ZnO and Mg-ZnO NPs

Analytical grade of Zinc chloride, magnesium chloride and sodium hydroxide were purchased from Merck, Mumbai, India. Double distilled water (DDW) was used to prepare the solution and dissolved Zinc Chloride and Sodium Hydroxide in 100 ml of double distilled water each for 1 hour using a magnetic stirrer. Then, the sodium hydroxide solution was added dropwise to the zinc chloride solution at room temperature and mixed well. The precipitate was separated and washed repeatedly with distilled water to remove unwanted impurities. Zinc chloride, magnesium chloride and

sodium hydroxide were dissolved in 100 ml double distilled water separately as above. A solution of zinc chloride and magnesium chloride was mixed together and stirred for about 2 hours. Finally, sodium hydroxide solution was added dropwise to the mixture and mixed well. It formed milky white precipitate of Mg-ZnO NPs after 30 minutes continuing the process. It was filtered and dried for further usage [5].

2.2. Characterization techniques and evaluation of antibacterial activities

Available characterization was performed according to literature [6]. The resulting ZnO and Mg-ZnO NPs were evaluated in antibacterial studies using the disc diffusion method. The antibacterial activity of the nanoparticles prepared in the course of this study against various bacteria was analyzed. An overnight culture of each organism was adjusted to an optical density of 0.1 and scraped on Mueller-Hilton agar plates. These plates were incubated at 37°C for 48 h. The inhibition zone diameter was measured in millimeters and images were recorded.

3. RESULTS AND DISCUSSION

3.1. Calculation of average crystalline size by XRD spectra

X-ray patterns of synthesized ZnO (a) and Mg-ZnO (b) nanoparticles (Fig. 1) have sharp and highly intense peaks. The indexed peaks are matched with JCPDS data (Card Nos.: 36-0451).

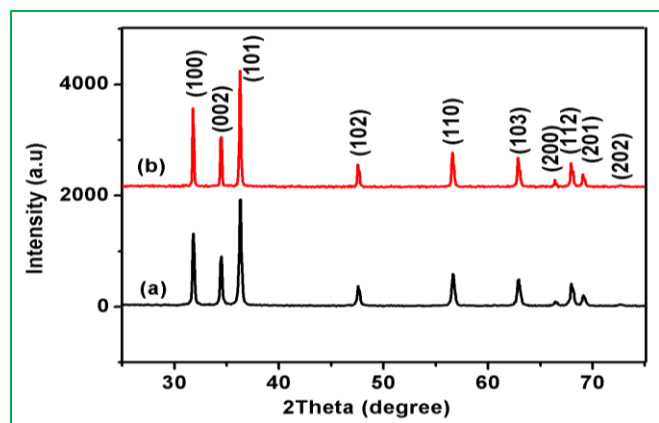


Fig. 1: XRD spectra of synthesized ZnO (a) and Mg-ZnO (b) NPs for average crystalline size

This is confirmed by the hexagonal structure of wurtzite with lattice parameters ($a = 3.2511$ and $c = 5.2076$ Å for ZnO). For Mg-ZnO, the hexagonal (wurtzite) properties of the crystal are also in good agreement with

the standard values and all the diffraction peak intensity increased due to the effect of higher Mg concentration 10 %. No secondary phase was observed in the samples (for comparison) as shown in Fig. 1a & b which suggested that Mg occupy the zinc sites in the Mg-ZnO NPs. The dominant (101) peak and its higher intensity indicated that the preferential growth of (101) orientation along c-axis for both NPs. The Debye-Scherrer formula [7] was used to calculate the average crystal size, which reached 51 and 42 nm for ZnO and Mg-ZnO respectively. The XRD results correlated well with better nanoscale antimicrobial activity.

3.2. Optical and photoluminescence spectra

UV-Vis. Spectra of ZnO (a) and Mg-ZnO (b) NPs (Fig. 2A) showed the peaks at 363 and 367 nm respectively. The small shift in the absorption peak is attributed to the doping of Mg to ZnO. Band gaps (E_g) of ZnO and Mg-ZnO NPs were of 3.23 and 3.20 eV. PL (emission) spectra of ZnO (a) and Mg-ZnO (b) NPs (Fig. 2B) have four main emission bands: a strong UV band at ~394 and 384 nm, a very weak green band at ~530 nm, a weak blue band at ~458 nm and a weak blue-green band at ~490 nm. Strong UV emission corresponds to exciton recombination associated with ZnO near-band edge emission. The faint blue and faded blue-green emissions may be due to surface defects in the NPs. The weak inexperienced band emission corresponds to the individually ionized gas vacancies of ZnO. This emission is due to the recombination of photogenerated holes in the single ionized charge state of certain defects. Compared with the Mg-ZnO NPs, the low green emission intensity from the ZnO NPNs could be due to the low density of empty oxygen during the preparation. The high UV emission intensity is of due to the high purity and perfect crystallization of the synthesized nanoparticles [8].

3.3. FTIR spectra

The appearance of band at 1041, 1404 and 1560 cm^{-1} could be attributed to C-O (stretching), C=O and C=C (asymmetric stretching) due to Lewis acidity and this C-O symmetric stretching due to Bronsted acidity group those are present on surface of the NPs in the citrates species. The Zn-O bonds were determined at 463 and 846 cm^{-1} which is of wurtzite structure. Due to the renovation of hydroxide to alkaline earth metal phase can transpire, Mg-ZnO NPs, Zn-O, O-H and C-H bonds have somewhat stretched. The results revealed that the present investigation were in agreement with past reports by researchers [9].

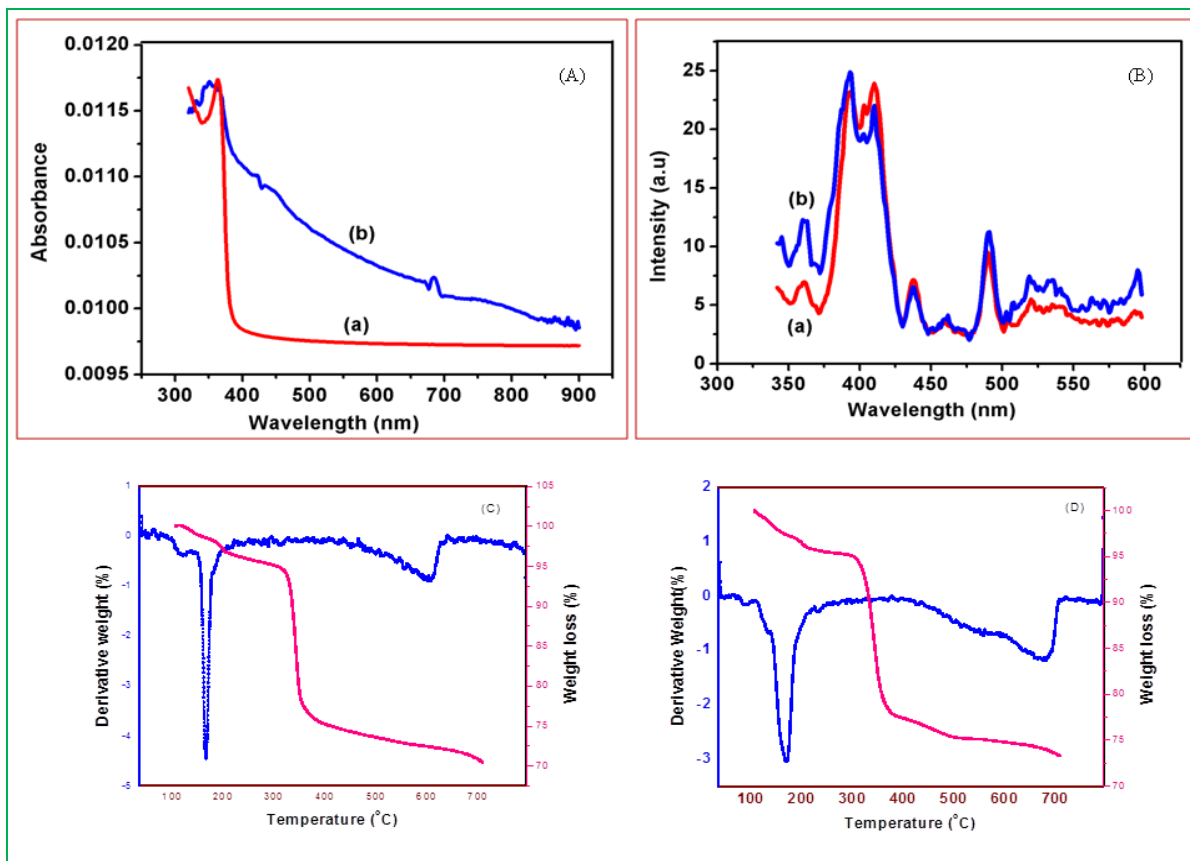


Fig. 2: Optical (A) spectra, PL (B) of synthesized ZnO (a) and Mg-ZnO (b) NPs and DTA/TGA of (C) ZnO and (D) Mg-ZnO NPs.

3.4. Thermal studies

DTA/TG studies of ZnO and Mg-ZnO are shown in Fig. 2C & D. By evaporation of inorganic materials, 100°C to 400°C the weight loss caused and the weight loss of the samples observed at room temperature to 100°C by evaporation of water molecules. The weight loss occurs due to the evaporation of unreacted materials after 400°C. At 465°C, the hydroxide to oxide is associated with the phase transformation of amorphous ZnO into its cubic phase. Transition occurs in the temperature range 37-65°C and 38-98°C with weight loss of 2 and 2.2 % in the TG thermogram of ZnO and Mg-ZnO NPs respectively in stage I. In DTA curves of ZnO and Mg-ZnO NPs, these weight losses are in the ranges 50°C and 88°C which attributed to the evaporation of water molecules. Transition occurs in the range 100-125°C and 112-175°C with weight loss of 2 and 15 % in the TG of ZnO and Mg-ZnO NPs in stage II and it conveyed by 115°C and 172°C in DTA curves of ZnO and Mg-ZnO NPs respectively. Then, loss of weight occurs in between 146-179°C and 283-324°C with weight loss of 18 and 2 % in TGA and their weight losses are accompanied by 116°C and 235°C in

DTA in stage III. In stage IV, transition occurs in the ranges 576-617°C and 379-436°C with weight loss of 2 and 2.2 % in TGA and it accompanied by 604°C and 400°C in DTA curves of ZnO and Mg-ZnO. Finally, stage V transition occurs in the range 540-652°C with weight loss of 17% in the TG of Mg-ZnO NPs. These weight losses are accompanied by 688°C in DTA curves of Mg-ZnO NPs. This transition is conveyed to evaporation of entire water molecules. The stable regions of ZnO NPs are enhanced by the ranges (177-288°C) while Mg-ZnO (198-296°C) [10].

3.5. Antibacterial activities of ZnO and Mg-ZnO NPs

The antibacterial studies of ZnO and Mg-ZnO (Fig. 3) NPs tested by disc diffusion method for 48 h against five different pathogenic bacteria's *Proteus vulgaris* (MTCC7299), *Escherichia coli* (ATCC25922), *Pseudomonas aeruginosa* (ATCC9027), *Klebsiella pneumonia* (MTCC13884) and *Staphylococcus aureus* (MTCC9886). The results revealed that, ZnO NPs have high antibacterial activity against *Escherichia coli* while Mg-ZnO NPs affects on the *Pseudomonas aeruginosa*.

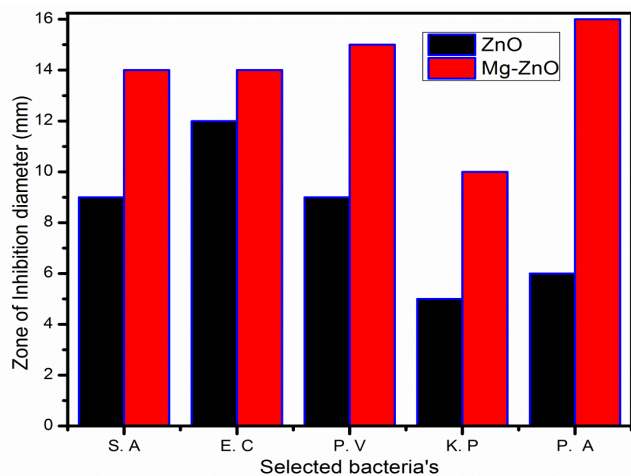


Fig. 3: Antibacterial studies of prepared (a) ZnO and (b) Mg-ZnO NPs

4. CONCLUSION

Mg-ZnO (Alkaline earth materials) and ZnO NPs were successfully synthesized. Mg-ZnO NPs have better the thermal stability region from (177-288°C) to (198-296°C). Optical properties and antibacterial efficiency were affected by size due to the influence of Mg-ZnO NPs. From the results, ZnO NPs have enhanced antibacterial activity against *Escherichia coli* and Mg-ZnO NPs on the *Pseudomonas aeruginosa*. The enhanced antibacterial activity of ZnO and Mg-ZnO NPs against selected bacteria's tackled in pharmaceutical, purification of water and conservative system with non-toxic.

Conflict of interest

None declared

Source of funding

None declared

5. REFERENCES

1. Pradeev Raj K, Sadaiyandi K, Kennedy A, Sagadevan S, Chowdhury Z, Johan MR, et al. *Nanoscale Res Lett*, 2018; **229**:1-13.
2. Jafar Ahamed A, Vijaya Kumar P, Karthikeyan M. *J Environ Nanotechnol*, 2016; **5**:11-16.
3. Zhang W, Tu G, Zhang H, Zheng Y, Yang L. *Mater Lett*, 2014; **114**:119-121.
4. Ramani M, Ponnusamy S, Muthamizhchelvan C, Cullen J, Krishnamurthy S, Marsili E. *Col Surf B: Biointer*, 2013; **105**:24-30.
5. Dhanalakshmi A, Palanimurugan A, Natarajan A. *Carb Pol*, 2017; **168**:191-200.
6. Dhanalakshmi A, Palanimurugan A, Natarajan B. *Mat Sci Engg C*, 2018; **90**:95-103.
7. Choi HH, Ollinger M, Singh RK. *Appl Phys Lett*, 2003; **82**:2494-2496.
8. Senthamilselvi V, Saravanakumar K, Jabena Begum N, Anandhi R, Ravichandran AT, Sakthivel B, et al. *J Mater Sci: Mater Electron*, 2012; **23**:302-308.
9. Fang J, Nakamura H, Maeda H. *Adv Drug Deliv Rev*, 2011; **63**:136-151.
10. Palanimurugan A, Kulandaisamy A. *J Organ Chem*, 2018; **861**:263-274.